Many-electron states of nitrogen-vacancy centers in diamond and spin density calculations

Ahmad Ranjbar,[1,*] Mohsen Babamoradi,[2] Mehdi Heidari Saani,[3,†] Mohammad Ali Vesaghi,[2]
Keivan Esfarjani,[4] and Yoshiyuki Kawazoe[1]

[1]*Institute for Materials Research, Tohoku University, Sendai 980-8577, Japan*
[2]*Department of Physics, Sharif University of Technology, P. O. Box 11365-9161, Tehran, Iran*
[3]*Physics Group, Maleke Ashtar University of Technology, P. O. Box 83145-115, Shahin Shahr, Iran*
[4]*Mechanical Engineering Department, Massachusetts Institute of Technology, Cambridge, Massachusetts 02139, USA*

(Received 17 February 2011; revised manuscript received 10 August 2011; published 25 October 2011)

Using a generalized Hubbard Hamiltonian, many-electron calculations of energy levels and corresponding wave functions of negatively charged and neutral nitrogen-vacancy centers in diamond were reported. The energies, orbital, and spin symmetries of the ground and excited states are in good quantitative agreement with available optical and electron paramagnetic resonance measurements. The many-electron wave functions were employed to predict the spin density on the N and C atoms in the ground and excited states. The present model explains the recent, experimentally observed definite nonzero spin density on N atom for the $^4A_2$ excited state of the neutral charge state of NV (NV^0) based on the multiple electronic configuration of the corresponding many-electron wave function.

DOI: 10.1103/PhysRevB.84.165212 PACS number(s): 71.70.Ej, 61.72.jn, 71.55.−i

I. INTRODUCTION

Nitrogen-vacancy (NV) center in diamond is a very rich system to study theoretically and to examine experimentally[1,2] various interesting physical phenomena such as spin-dependent photoluminescence,[3] electron paramagnetic resonance (EPR),[4,5] spin-orbit interaction of unpaired electrons,[3,6,7] uniaxial strain effect on optical transitions,[8] dynamic Jahn-Teller effect in the ground and excited states,[8,9] hole burning,[10] and so on. Employing such interesting physical phenomena to implement a solid-state qubit is currently an active research field.[11] Now, the accepted idea is that the negatively charged state of NV (NV^-) is responsible for the observation of such interesting phenomena.[12] This center has a strong optical transition with a zero phonon line (ZPL) at 1.945 eV.[2] The excited-state structure of the defect is not yet fully known, which hinders the understanding of the spin-flip fluorescence of the NV center.[13] The general idea is that the spin polarization via optical excitation is initialized through intersystem crossing (ISC) between spin triplet states and a singlet state and is induced by spin-orbit interaction.[3] There is disagreement in the symmetry and energy levels of the ground and excited states which involve the intersystem crossing.[12,14,15] Recently, the neutral charge state of NV (NV^0) has been also studied.[6] This center has an optical transition with a ZPL at 2.156 eV.[8] Felton *et al.* reported an EPR signal from a center with $S = 3/2$ and C_{3v} symmetry under light illumination indicating that the signal comes from an excited state.[6] Simple electronic structure arguments suggest that EPR signal arises from a low lying $^4A_2$ excited state of the NV^0, which is derived from the $a_{1N}^2 a_{1C}^1 e^2$ electronic configuration, where a_{1N} and a_{1C} are dangling orbitals localized on the nitrogen and carbon atoms, respectively.[6] From hyperfine interaction (HFI) data, they measured a definite nonzero spin density on N atom for the $^4A_2$ excited state of the NV^0 by EPR, which is in disagreement with the preassumed $a_{1N}^2 a_{1C}^1 e^2$ electronic configuration of $^4A_2$. This configuration gives zero spin density on neighboring N atom.[6] Gali *et al.* used *ab initio* supercell calculations and concluded that negligible spin density is expected for the ^2E ground state but considerable spin polarization may be expected for the $^4A_2$ excited state.[16] They adjusted the nonzero spin of Felton *et al.*[6] analysis with the possible hybridization of both a_{1N} and a_{1C} defect orbitals. Unlike the ground state of NV^-, the EPR signal of the $S = 1/2$ ^2E ground state of the NV^0 has not been detected so far.[6] Uniaxial stress-splitting study of the ZPL[8] and arguments of simple electronic structure result in assignment of ^2E to the ground state and $^2A_1$ to the excited state of NV^0. The lack of EPR detection for the ground state of NV^0 is likely to be due to dynamic Jahn-Teller coupling, which broadens the EPR lines and dramatically reduces the detection sensitivity.[6]

Generally, there have been two groups of approaches to electronic structure of NV. In the first group of approaches, localized models[17,18] are used and in the second ones, extended models are employed.[12,14,15] In the first group, the electrons of the broken bonds, which are in the C_{3v} symmetric local potential of the vacant site, are considered as an isolated molecule. Since these groups of approaches are restricted to a few atoms, many-body techniques such as configuration interaction (CI) and generalized Hubbard Hamiltonian are applicable.[19,20] In the second group, i.e., extended models, the effect of the remaining part of the lattice on the vacancy is more important. The vacancy is modeled as a missing atom in a supercell with few hundreds atoms. Due to considering a lager set of atoms around the vacant site, single-particle techniques are usually employed. The similarity between these two categories is in their group theoretical aspects for accounting symmetries of the system, while their main difference is in the importance of electron-electron (e-e) correlation effects. Since the localized models have been restricted to the first neighboring atoms, spin density distribution on the farther neighboring atoms and its interaction with NV electrons could not be evaluated.

In this paper, a new set of computed many-electron energy levels and corresponding many-electron wave functions of NV centers are reported. Our model is able to calculate the contribution of each available multiple electronic configuration to the

many-electron states. The sequence and energies of the ground and excited many-electron states are presented and compared to the previous works. We discuss the energy of the singlet level, which involves the ISC of NV^- and also the position of experimentally detectable $^4A_2$ excited state of NV^0 by EPR. From the calculated wave functions, we have been able to estimate the spin density on neighboring N and C atoms in the ground and excited states of the NV^- and NV^0. Particularly, the computed value of spin density on N atom for the $^4A_2$ excited state of NV^0 from multiple electron configurations of the wave function is in fair agreement with experiment. The results are compared with available EPR measurement data. Additionally, the spin densities are predicted and discussed for the states that have not been detected so far by EPR.

II. CALCULATION METHOD

The nitrogen-vacancy center consists of a substitutional nitrogen atom next to a carbon vacancy. It has trigonal (C_{3v}) symmetry around the crystallographic ⟨111⟩ axes connecting the nitrogen and the vacant place (see Fig. 1). We performed a precalculation on single-electron wave functions (dangling orbitals)[21] of NV with a DFT method using B3LYP functional and 6–31G basis set implemented in the Gaussian 2003 package.[22] A H-terminated $C_{71}H_{85}$ molecular diamond cluster including a NV center was allowed to relax and employed to model the NV center in the lattice. As a result, the neighboring nitrogen and three carbon atoms of NV^-(NV^0) were observed to relax outward from the defect center as 9% (8.5%) and 5% (6%), respectively. A similar DFT cluster method with almost the same cluster size and basis set has been successfully applied to model vacancy-related defects in diamond.[12,21] Since we performed a spin-dependent calculation with $S = 1$ and $1/2$ for the ground states of NV^- and NV^0, respectively, the highest occupied molecular Kohn-Sham orbitals (HOMO) of the relaxed structures had spin up $(+1/2)$ with an expansion on the atomic orbitals of the clusters. The single-electron wave functions or dangling orbitals φ_i and φ_j corresponding to each neighboring atoms of NV in Fig. 1, were extracted from the HOMO wave functions expanded on each neighboring atoms and its six back-bond neighbors. The tail of the NV electrons on the fourth neighboring shell and farther atoms has been neglected and finally the constructed wave function was normalized. A set of different basis sets and cluster sizes reproduce similar HOMO orbitals. In the early many-body calculation for an isolated vacancy in diamond, simple undisturbed sp^3 orbitals were used to calculate the φ_i.[17]

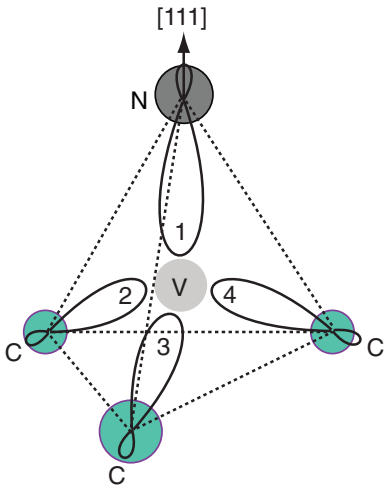

FIG. 1. (Color online) C_{3v} symmetry of the NV defect and its dangling orbitals labeled as 1 for N and 2, 3, and 4 for C atoms considered in the present study.

The following methodology is used to calculate many-electron states of NV defect. Electron-electron and electron-ion interactions are modeled by a generalized form of Hubbard Hamiltonian, which takes into account all Coulomb and exchange terms of e-e interactions as follows:[18,19]

$$H = \sum_{ij\sigma} t_{ij} c^\dagger_{i\sigma} c_{j\sigma} + \sum_i U_i n_{i\uparrow} n_{i\downarrow} + \frac{1}{2} \sum_{i\neq j,\sigma\sigma'} V_{ij} n_{i\sigma} n_{j\sigma'} + \frac{1}{2} \sum_{ijlm,\sigma\sigma'} X_{ijlm} c^\dagger_{i\sigma} c^\dagger_{j\sigma'} c_{m\sigma'} c_{l\sigma}. \quad (1)$$

In Eq. (1), i, j, l, and m are dangling atomic orbital indices around the NV center, ranging from one (N atom) to four (three C radicals) as shown in Fig. 1. σ and σ' are the spin indices that could be up and down and c and $c^\dagger$ are annihilation and creation operators, respectively. In Eq. (1), t_{ij} represents the hopping or kinetic and electron-ion terms and is computed by Eq. (2) in atomic units.

$$t_{ij} = \int \varphi^*_i(r) \left[-\frac{1}{2}\nabla^2 + V(r) \right] \varphi_j(r) d^3r, \quad (2)$$

where $\varphi_i(r)$ and $\varphi_j(r)$ are the dangling orbitals of NV obtained from the single-electron DFT calculations as previously explained in this section. The Coulomb interaction parameters in Eq. (1) are defined from following equation in atomic units:

$$X_{ijlm} = \int \varphi^*_i(r) \varphi^*_j(r') \frac{1}{|r - r'|} \varphi_l(r) \varphi_m(r') d^3r\, d^3r'. \quad (3)$$

X_{ijlm} of Eq. (3) with equal indices (X_{iiii}) is U_i, the intersite direct Coulomb e-e interaction, X_{ijlm} of Eq. (3) with two equal pair indices meaning X_{ijij} or V_{ij} is the intrasite direct Coulomb interaction and the remaining X_{ijlm} of Eq. (3) are the exchange part of e-e interaction. The computed parameters for NV^- and NV^0 are summarized in Table I.

If we index the nitrogen site as 1 and the three adjacent carbon sites as 2, 3, and 4, the trigonal C_{3v} symmetry of the defect (see Fig. 1) reduces the number of t_{ij} parameters of Eq. (2) to four, the number of U_i parameters to two, the number of V_{ij} to two, and the number of X_{ijlm} to twelve in Table I. Similar approach has been successfully applied to calculate many-electron energy levels and wave functions of the isolated vacancy in diamond.[18,19] The constructed generalized Hubbard Hamiltonian for modeling diamond vacancies allows for a unified and accurate treatment of many-electron energy levels and wave functions for both charge states of NV defect. The resulting wave functions are exact eigenfunctions of the Hamiltonian. Due to computational limitations, we only consider the first neighboring atoms around the defect since the extension of such many-body basis set to farther atoms is too demanding. We considered five and six electrons for the NV^0 and NV^-, respectively. By considering electron's spin in

TABLE I. The computed values of the parameters of generalized Hubbard Hamiltonian of Eq. (1) for NV^- (NV^0) using single-electron DFT wave functions.

t_{11}	t_{ii}	t_{1i}	t_{ij}	U_1	U_i	V_{i1}	V_{ij}	X_{1ii1}	X_{ijji}
−2.73 (−2.72)	−7.59 (−7.56)	−2.97 (−2.95)	−3.68 (−4.18)	10.8 (7.34)	3.54 (11.77)	5.66 (3.909)	0.02 (5.819)	0.10 (0.011)	0.10 (0.12)
X_{111i}	X_{iii1}	X_{iiij}	X_{11ij}	X_{ii1j}	X_{iijk}	X_{1i1j}	X_{i1ij}	X_{ijik}	X_{1ijk}
0.034 (0.066)	0.14 (0.15)	0.68 (0.80)	0.01 (0.009)	0.0007 (0.015)	−0.03 (−0.041)	0.239 (0.318)	0.279 (0.296)	−0.003 (−0.022)	−0.017 (−0.017)

the Fock space representation, the many-electron basis of the Hilbert space was constructed as

$$|\psi_i\rangle = |a_{i1}a_{i2}\cdots a_{i8}\rangle, \tag{4}$$

where a_{i1} to a_{i8} are -1, $+1$, or zero (for spin down, spin up, and without an electron on site i, respectively). These numbers represent the occupation condition of four neighboring sites of NV center. The Hamiltonian calculation has been carried out in S_z representation of basis set in Eq. (4). In parallel, we calculated the square of total spin S^2 operator of 6 (5) electrons of NV^-(NV^0) in S_z representation of basis in Eq. (4). The unitary matrix U transforms the Hamiltonian of Eq. (1) from S_z basis representation ($H_{\{S_z\}}$) to S^2 basis representation ($H_{\{S^2\}}$). U was constructed from the eigenvectors of the S^2 matrix and the transformation was carried out via $H_{\{S^2\}} = U^\dagger H_{\{S_z\}} U$. After transformation, we had $[H_{\{S^2\}}, S^2] = 0$, hence by exact diagonalization of $H_{\{S^2\}}$, complete eigenstates of the Hamiltonian with proper S and S_z values were obtained. Resulting eigenfunctions of the Hamiltonian $|\Psi^j\rangle$ as Eq. (5),

$$|\Psi^j\rangle = \sum_{i=1}^{N} \alpha_i^j \, |\psi_i\rangle \tag{5}$$

are a linear combination of basis set $|\psi_i\rangle$ of Eq. (4) with definite spin and symmetry degeneracy. For the neutral and negatively charged NV centers, there are C(8,5) = 56 and C(8,6) = 28 states of Eq. (4), respectively, in the Fock space representation. Hence index i in Eq. (5) goes from 1 to 56 and from 1 to 28, for NV^0 and NV^- centers, respectively. In order to calculate spin density on a specific neighboring atom of the NV, for example, site m (m can be a site of N or one of C atoms) in a specific many-electron state $|\Psi^j\rangle$, we identified such $|\psi_i\rangle$ in expansion of Eq. (5) in which only one electron occupies the site m. If one of the a_{i1} or a_{i2} in Eq. (4) is zero then m represents N site and similarly for other a_{i3}–a_{i8}, m represents a specific carbon sites. The total sum of squares of corresponding coefficients $(\alpha_i^j)^2$ of such $|\psi_i\rangle$, which have one electron on site m was evaluated to obtain the spin density on this site.

III. MANY-ELECTRON ENERGY LEVELS

The calculated many-electron energy levels of the NV^- have been shown in Fig. 2. From Fig. 2, the ground state of the NV^- is $^3A_2$ and the next excited states are ^1E, $^1A_1$, ^3E, ^1E, and $^1A_1$, respectively. Since in our model the change of atomic structure during excitation is neglected, the calculated vertical excitation energy differs from ZPL energy.[23] From Fig. 2, the energy difference between levels involved in $^3A_2$ to ^3E optical transition is 2.38 eV, this value is 0.18 eV larger than the experimental value of 2.20 eV (see Ref. 2) for vertical excitation energy. The $^3A_2$ ground state has been observed in EPR experiment.[4] Recently, the electronic structure of the ^3E excited state has been studied as a function of local strain, combining resonant excitation and optically detected magnetic resonance, which indicates that the excited state of the NV^- splits to six sublevels.[24] Using spin-polarized local density functional cluster theory, Goss *et al.*[12] calculated the energy-level ordering of NV^- center as $^3A_2$, ^1E, $^1A_1$, and ^3E with an energy difference of 1.77 eV for the ZPL of optical absorption line 1.945 eV. Unlikely, in another study by Gali *et al.*,[14] using a different variation in DFT calculations, the energy levels were found to be $^3A_2$, $^1A_1$, ^1E, and ^3E with the value of 1.71 eV for the ZPL of optical absorption line 1.945 eV. Delaney *et al.*[20] used the CI calculation for a larger cluster, such as $C_{284}H_{144}N^-$, and found a difference of energy of $^3A_2$ and ^3E as 1.90 eV for the ZPL of optical absorption line 1.945 eV. Zyubin and his coworkers[25] used a Hartree-Fock-CI method to calculate the energy levels of the NV for different H-terminated clusters. They found the energy-level order for NV^- as $^3A_2$, ^1E, $^1A_1$, ^3E, ^1E, $^1A_2$, ^3E, and ^1E, in agreement with our finding in Fig. 2. In the work of Zyubin *et al.*,[25] by averaging over different calculated results, the ^1E energy level is about 0.8 eV above the ^3E state. Our results in Fig. 2 reveal that there is a ^1E state, which is about 2.2 eV above the

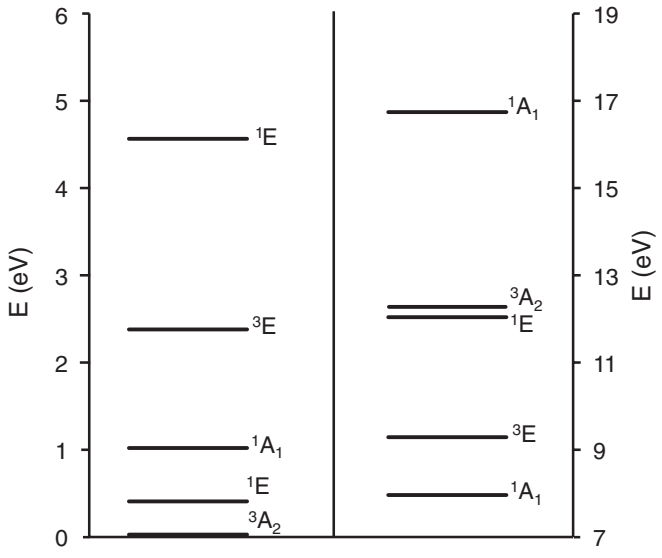

FIG. 2. Many-electron energy levels of the NV^- center in diamond.

^{3}E state. We suggest that the ^{1}A$_1$ singlet level is more likely responsible for the intersystem crossing mechanism with the ^{3}E excited state. Recently, the light polarization dependence of 1042 nm (1.19 eV) absorption confirms that the transition is between orbitals of A and E character.[26] In our results (see Fig. 2), there are upper ^{1}A$_1$ and lower ^{1}E states with an energy difference of 0.61 eV. Until now, however, most investigations of the NV center have been limited to DFT, the ability of which to describe the excited states is questionable.[15] Moreover, DFT is a single-electron theory, therefore its results can only be used to estimate the sequence of levels.[15] As a consequence, more recently, Ma *et al.*[15] applied *ab initio* many-body perturbation theory (MBPT) and found the sequence of the energy levels as ^{3}A$_2$, ^{1}E, ^{1}A$_1$, ^{3}E, and ^{1}E$'$. The sequence and energy levels are in agreement with our results except their ^{1}E$'$ energy level, which is very close to the ^{3}E excited state of the NV$^-$. Gali *et al.*[14] suggest that the singlet ^{1}E$'$ state can be involved in the intersystem crossing mechanism.

Additionally, the calculated many-electron energy levels of the NV^0 have been shown in Fig. 3. From Fig. 3, the ground state of NV^0 is ^{2}E and the next excited states are ^{4}A$_2$, ^{2}A$_1$, ^{2}E, ^{2}A$_1$, and ^{2}E, respectively. The previous uniaxial stress-splitting study of ZPL[8] and arguments of simple electronic structure result in assignment of ^{2}E to the ground and ^{2}A$_1$ to the optically excited states.[6] Our computed vertical excitation energy[23] for ^{2}E to ^{2}A$_1$ transition is 2.64 eV.[8] Goss *et al.*[12] calculated ZPL energy for ^{2}E to ^{2}A$_1$ transition as 1.57 eV, 0.59 eV smaller than the experimental value of 2.156 eV. Using different clusters and Hartree-Fock-CI method, Zyubin *et al.*[25] found the energy levels of NV^0 as ^{2}E, ^{2}A$_2$, ^{2}E, ^{2}A$_1$, and ^{2}E. In the case of NV^0, only the low lying ^{4}A$_2$ state has been detected by EPR experiment under optical pumping.[6] Gali *et al.*[16] used *ab initio* supercell method and computed ^{4}A$_2$ excited state of the NV^0 with a larger energy by about 0.86 eV compared with that of the low-symmetry ^{2}E ground state. In our model, this state is 0.67 eV above the ground state and can be populated through nonradiative decay of the excited state ^{2}A$_1$ to the ground state ^{2}E via this intermediate state.

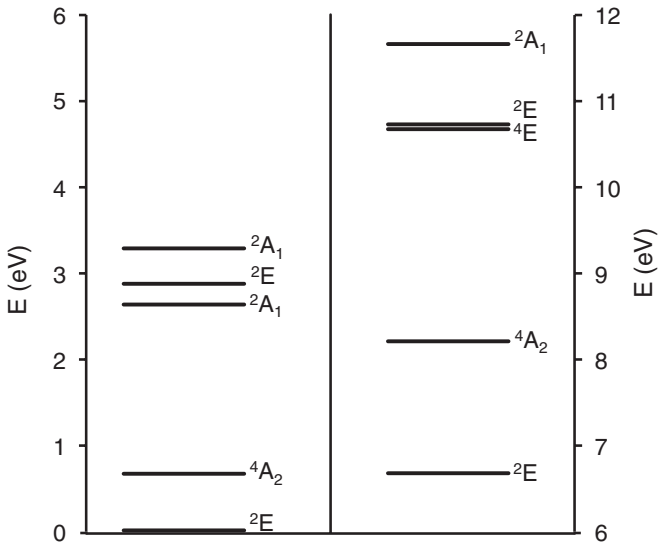

FIG. 3. Many-electron energy levels of the NV^0 center in diamond.

TABLE II. Calculated spin densities on the neighboring N and C atoms of NV$^-$ for the many-electron ground and excited states.

State	Energy (eV)	S_z	N	C_1	C_2	C_3
$^3A_2$(GS)	0.00	0, ± 1	0.00	0.33	0.33	0.33
^1E	0.41	0	0.01	0.25	0.19	0.42
$^1A_1$	1.03	0	0.01	0.20	0.20	0.20
^3E	2.38	0, ± 1	0.23	0.27	0.40	0.11
^1E	4.57	0	0.37	0.04	0.08	0.24
$^1A_1$	7.98	0	0.31	0.12	0.12	0.12
^3E	9.31	0, ± 1	0.27	0.16	0.41	0.16
^1E	12.06	0	0.12	0.09	0.07	0.09
$^3A_2$	12.30	0, ± 1	0.50	0.17	0.17	0.17
$^1A_1$	16.76	0	0.03	0.10	0.10	0.10

IV. SPIN DENSITY ON NEIGHBORING ATOMS

Using wave functions of each many-electron state of the NV^0 and NV$^-$, we calculated spin density on the neighboring N and C atoms. The results being summarized in Tables II and III, respectively. One of the most important outcomes of EPR experiments on NV centers is obtaining the spin density on the neighboring sites of such centers.[6] The ^{3}A$_2$ ground and ^{3}E excited states of the NV$^-$ have nonzero spin and, in principle, can be observed by EPR experiment. Due to maximum population at thermal equilibrium, it is more straightforward to measure the spin of the ground state. The spin of other excited states can be observed under optical pumping, provided that the transition to the excited state is optically allowed or the excited state is a low-lying state with considerable lifetime. According to Table II, in the ground state ^{3}A$_2$, the spin density on the N atom is absolutely zero and the spin density has been equally distributed on the three neighboring C radicals. By going to the first and second excited states (^{1}E and ^{1}A$_1$) the spin density on N remains negligible, whereas, there is a spin density redistribution between three neighboring C radicals. In the optically allowed ^{3}E excited state, there is a significant enhancement of 23% of the spin density on the N atom and, consequently, a reduction in the spin density on the three neighboring C radicals. For the ^{3}A$_2$

TABLE III. Calculated spin densities on the neighboring N and C atoms of NV^0 for the many-electron ground and excited states.

State	Energy (eV)	S_z	N	C_1	C_2	C_3
^2E(GS)	0.00	$\pm\frac{1}{2}$	0.04	0.28	0.38	0.30
$^4A_2$	0.68	$\pm\frac{3}{2}, \pm\frac{1}{2}$	0.19	0.27	0.27	0.27
$^2A_1$	2.64	$\pm\frac{1}{2}$	0.30	0.23	0.23	0.23
^2E	2.88	$\pm\frac{1}{2}$	0.30	0.22	0.33	0.15
$^2A_1$	3.29	$\pm\frac{1}{2}$	0.50	0.17	0.17	0.17
^2E	6.68	$\pm\frac{1}{2}$	0.25	0.22	0.12	0.41
$^4A_2$	8.21	$\pm\frac{3}{2}, \pm\frac{1}{2}$	0.14	0.29	0.29	0.29
^4E	10.73	$\pm\frac{3}{2}, \pm\frac{1}{2}$	0.33	0.32	0.13	0.22
^2E	10.75	$\pm\frac{1}{2}$	0.09	0.30	0.14	0.47
$^2A_1$	11.67	$\pm\frac{1}{2}$	0.12	0.29	0.29	0.29

ground state of NV^-, He *et al.*[3] were able to account for 72% of the spin density as being localized in the dangling bonds on the three neighboring carbon atoms of the vacancy. Only about 0.2% of the wave function was accounted for nitrogen. The remaining 28% of the wave function was presumably spread over more distant carbon neighbors.[3] Tucker and coworkers[27] showed that the ^{14}N quadrupole parameter is a measure of the unpaired-electron population in a $2p$ orbital on the nitrogen atom. In their study, the value of quadrupole parameter implies that less than 2% of unpaired electron probability density is located on the nitrogen atom or that unpaired electron probability density is mainly localized in the dangling orbital of the three carbon atoms around the vacancy. Felton *et al.*[6] used ^{13}C hyperfine interaction and showed that these results can also be concluded from the hyperfine interaction. Also, by assuming that one-third of unpaired-electron probability density is localized on each of the carbon atoms neighboring the vacancy, they found that the two sets of carbon neighbors account for 96% of the unpaired-electron probability density for NV^-, with ∼84% on the three nearest carbon atoms from the vacancy. The experimental hyperfine interaction parameters (A_{11}, A_{22}, A_{33}) for N atom is not zero (around 2 MHz) whereas the corresponding values for the three neighboring C atoms of NV are 120–200 MHz.[1,7] Therefore HFI parameters of N atom are between 1–2% of the ones for C atoms and even less than 15% of the HFI parameters of farther C atoms. Gali *et al.*[14] performed an all-electron calculation, which can account small contribution of core electrons of N to the hyperfine interaction tensor and explained the nonzero, small amount of HFI parameter on neighboring N atom. Our calculated zero spin density on the N atom is in very good agreement with the very small, measured HFI parameter reported by EPR.[1,7] It should be noted that our model is restricted to valence electrons and cannot consider the polarization probability of core-electron wave function. There are a few experimental works on the excited state of NV^-,[9,24,28,29] which use local strain field and spin sublevel transitions to explain low-temperature and room-temperature excitation spectra. Gali *et al.*[30] found that the spin density apparently is enhanced a lot around the N atom, while it dropped around the C atoms. In other words, the spin density is mostly redistributed between the N atom and the three C atoms upon excitation. From Table II, we are able to obtain 23% of spin density migration from the C toward N atom by optical excitation. The spin densities on each neighboring atom of NV^0 for the ground and excited states are listed in Table III. The ground and excited states as well as the low-lying $^4A_2$ have nonzero spin and, in principle, can be observed by the EPR experiment. Similar to NV^-, in the ^2E ground state, the spin density on the N atom is negligible (4%) and in excited states the spin density migrates from the C radicals toward the N atom. By going to the first excited states ($^4A_2$), the spin density on N enhances. In the optically allowed $^2A_1$ excited state, there is a significant enhancement of 30% of the spin density on the N atom and, consequently, a reduction in the spin density on the three neighboring C radicals. From Table III, we are able to obtain 26% of spin density migration from the C toward N atom by optical excitation. Since the spin of the low-lying $^4A_2$ excited state differs from the ^2E ground state, radiative decay is forbidden and therefore the $^4A_2$ excited state would be a long-lived state. The enhanced lifetime of $^4A_2$ allows this state to be detected by the EPR under optical illumination.[6] Felton *et al.*[6] detected an EPR signal with $S = 3/2$ and a trigonal symmetry. The measured hyperfine interaction,[6] indicates that there is a small but significant localization of the unpaired electron density on the nitrogen. This signal was attributed to the $^4A_2$ excited state of NV^0. The results indicate that approximately 6% of the unpaired electron probability density is localized on the nitrogen, which is much larger than for the $^3A_2$ ground state of NV^-.[3] Felton *et al.*[6] discuss that the $^4A_2$ state can be derived from $a_{1N}^2 a_{1C}^1 e^2$ and $a_{1N}^1 a_{1C}^2 e^2$, but in the first configuration the unpaired electron probability density is expected to be predominately localized in the carbon dangling orbitals surrounding the vacancy and in the second, there is a significant unpaired electron probability density on the nitrogen resulting in a large nitrogen hyperfine interaction. This is not likely, but it is probable that there is a mixing of the a_{1N} and a_{1C} one-electron levels and this gives rise to the observed nitrogen hyperfine interaction.[6] Gali *et al.*[16] considered the possibility of hybridization of both a_{1N} and a_{1C} defect orbitals and adjusted Felton *et al.*'s[6] analysis by obtaining considerable spin polarization for the $^4A_2$ excited state and a negligible spin density for the ^2E ground state. It may be not trivial that ^2E ground state of NV^0 is from single Slater determinant.[16] Anyhow, considering a single Slater determinant to describe the wave function of the $^4A_2$ does not regenerate the small nonzero (6%) amount of spin density reported by EPR. Our calculated many-body wave function of $^4A_2$ consists of many electronic configurations or Slater determinant. Our calculated spin density on the N atom in the $^4A_2$ state of NV^0 is 19%, in fair agreement with Felton *et al.* reported EPR data.[6] This value is also much larger than the calculated spin density in the ground state of the NV^-, which is 0%. Since our Fock space basis set is only restricted to the four neighboring atoms, the delocalization of dangling orbital wave functions to farther atoms is indirectly included in our Hubbard-Hamiltonian parameters calculations. Electron delocalization to farther atoms is included in the DFT calculation of single electron wave functions $\varphi_i(r)$, which is extended up to the fourth shell of neighboring atoms. In other words, the effect of delocalization in practice reduces the value of Hamiltonian parameters, which are computed from $\varphi_i(r)$ using Eqs. (2) and (3). Due to the limitation of our calculations to the first neighboring atoms, we expect that the calculated 19% spin density on N for $^4A_2$ should be slightly larger than the experimental value. It is important to notice that the Kohn-Sham LDA spin density approximates the many-body spin density where the exchange and correlation between the noninteracting Kohn-Sham particles is taken into account. In the present work frame, many Slater determinants are needed in order to consider correlation effects. The percentages of each electronic-configuration contribution to the $^4A_2$ state are shown in Fig. 4. The possible electronic configurations of five electrons of NV^0 that are distributed on four surrounding dangling orbitals in the $^4A_2$ excited state are (2,111), (1,211), (1,121), and (1,112). In this notation, the first number in parenthesis represents the number of electrons on N atom and the other three numbers in paranthesis are the number of electrons on C atoms. From Fig. 4, the contribution of (2,111) electronic configuration that has zero spin on N to the

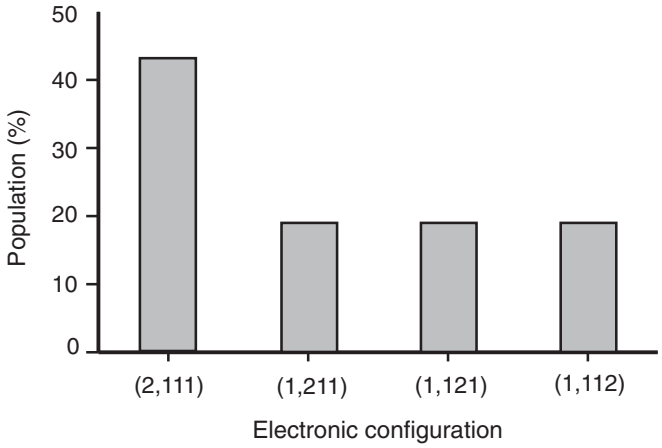

FIG. 4. The population of each possible electronic configuration that contributes to the many-body wave function of $^4A_2$ of NV^0.

many-body wave function is 43%, whereas the contribution of other electronic configurations with distributed spin between N and C atoms to the wave function is 19%. This is in fair agreement with the EPR finding[6] and in good agreement with Gali *et al.*'s[16] conclusion about spin density in the $^4A_2$ state.

V. CONCLUSION

In conclusion, the calculated energies, orbital and spin symmetries of many-electron states of NV^- and NV^0 are in agreement with the EPR, optical excitation, and luminescence measurements. The energy of the low-lying $^1A_1$ excited state of NV^-, which most likely involves the ISC, was obtained. From many-electron wave functions, the spin density on the N and C atoms was calculated for the ground and excited states and the results were in good agreement with the measured spin density by EPR in the $^3A_2$ ground state of the NV^-. The results, generate the small, nonzero spin density on N atom for the $^4A_2$ excited state of the NV^0 reported by EPR. We also predicted the spin densities on neighboring atoms of NV^- and NV^0 in many-electron excited states that have not been detected by EPR so far.

ACKNOWLEDGMENTS

The authors gratefully acknowledge the Center for Computational Materials Science at the Institute for Materials Research, Tohoku University, for use of the Hitachi SR11000 (Model K2) supercomputer system. A. Ranjbar thanks the Global COE Program "Materials Integration (International Center of Education and Research), Tohoku University," MEXT, Japan for financial support.

*ranjbar@imr.edu
†Corresponding author: heydaris@yahoo.com

[1] J. H. N. Loubser and J. A. van Wyk, Rep. Prog. Phys. **41**, 1201 (1978).
[2] G. Davies and M. F. Hamer, Proc. R. Soc. London A **348**, 285 (1976).
[3] X. F. He, N. B. Manson, and P. T. H. Fisk, Phys. Rev. B **47**, 8809 (1993).
[4] J. H. N. Loubser and J. A. van Wyk, in *Diamond Research 1977*, edited by P. Daniel, pp. 11–14.
[5] D. A. Redman, S. Brown, R. H. Sands, and S. C. Rand, Phys. Rev. Lett. **67**, 3420 (1991).
[6] S. Felton, A. M. Edmonds, M. E. Newton, P. M. Martineau, D. Fisher, and D. J. Twitchen, Phys. Rev. B **77**, 081201(R) (2008).
[7] S. Felton, A. M. Edmonds, M. E. Newton, P. M. Martineau, D. Fisher, D. J. Twitchen, and J. M. Baker, Phys. Rev. B **79**, 075203 (2009).
[8] G. Davies, J. Phys. C **12**, 2551 (1979).
[9] G. D. Fuchs, V. V. Dobrovitski, R. Hanson, A. Batra, C. D. Weis, T. Schenkel, and D. D. Awschalom, Phys. Rev. Lett. **101**, 117601 (2008).
[10] N. R. S. Reddy, N. B. Manson, and E. r. Krausz, J. Lumin. **38**, 46 (1987).
[11] R. J. Epstein, F. M. Mendoza, Y. K. Kato, and D. D. Awschalom, Nat. Phys. **1**, 94 (2005).
[12] J. P. Goss, R. Jones, S. J. Breuer, P. R. Briddon, and S. Öberg, Phys. Rev. lett. **77**, 3041 (1996).
[13] N. B. Manson, J. P. Harrison, and M. J. Sellars, Phys. Rev. B **74**, 104303 (2006).
[14] A. Gali, M. Fyta, and E. Kaxiras, Phys. Rev. B **77**, 155206 (2008).
[15] Y. Ma, M. Rohlfing, and A. Gali, Phys. Rev. B **81**, 041204 (2010).
[16] A. Gali, Phys. Rev. B **79**, 235210 (2009).
[17] C. A. Coulson and M. J. Keasley, Proc. R. Soc. London A **241**, 433 (1957).
[18] M. Heidari Saani, M. A. Vesaghi, K. Esfarjani, T. Ghods Elahi, M. Sayari, H. Hashemi, and N. Gorjizadeh, Phys. Rev. B **71**, 035202 (2005).
[19] M. Heidari Saani, M. A. Vesaghi, K. Esfarjani, and A. Shafiekhani, Diam. Relat. Mater. **13**, 2125 (2004).
[20] P. Delaney, J. C. Greer, and J. A. Larsson, Nano Lett. **10**, 610 (2010).
[21] M. Heidari Saani, H. Hashemi, A. Ranjbar, M. A. Vesaghi, and A. Shafiekhani, Eur. Phys. J. B **65**, 219 (2008).
[22] M. J. Frisch *et al.*, GAUSSIAN 03, revision C.02, Gaussian Inc., Willingford, CT, 2004.
[23] A. Gali, E. Janzen, P. Deak, G. Kresse, and E. Kaxiras, Phys. Rev. Lett. **103**, 186404 (2009).
[24] A. Batalov, V. Jacques, F. Kaiser, P. Siyushev, P. Neumann, L. J. Rogers, R. L. McMurtrie, N. B. Manson, F. Jelezko, and J. Wrachtrup, Phys. Rev. Lett. **102**, 195506 (2009).
[25] A. S. Zyubin, A. M. Mebel, M. Hayasht, H. C. Chang, and S. H. Lin, J. Comput. Chem. **30**, 119 (2009).
[26] V. M. Acosta, A. Jarmola, E. Bauch, and D. Budker, Phys. Rev. B **82**, 201202 (2010).
[27] O. D. Tucker, M. E. Newton, and J. M. Baker, Phys. Rev. B **50**, 15586 (1994).
[28] P. Neumann, R. Kolesov, V. Jacques, J. Beck, J. Tisler, A. Batalov, L. Rogers, N. B. Manson, G. Balasubramanian, F. Jelezko, and J. Wrachtrup, New J. Phys. **11**, 013017 (2009).
[29] B. Smeltzer, L. Childress, and A. Gali, New J. Phys. **13**, 025021 (2011).
[30] A. Gali, Phys. Rev. B. **80**, 241204(R) (2009).